MOX-Report No. 01/2016

Computational fluid-dynamic analysis of carotid bifurcations after endarterectomy: closure with patch graft versus direct suture

Domanin, M.; Buora, A.; Scardulla, F.; Guerciotti, B.;

Forzenigo, L.; Biondetti, P.; Vergara, C.

MOX, Dipartimento di Matematica
Politecnico di Milano, Via Bonardi 9 - 20133 Milano (Italy)

mox-dmat@polimi.it http://mox.polimi.it

COMPUTATIONAL FLUID-DYNAMIC ANALYSIS OF CAROTID BIFURCATIONS AFTER ENDARTERECTOMY: CLOSURE WITH PATCH GRAFT VERSUS DIRECT SUTURE

Maurizio Domanin [a b]
a Operative Unit of Vascular Surgery, Fondazione I.R.C.C.S. Ca' Granda Ospedale Maggiore Policlinico di Milano, Italy,
b Department of Clinical Sciences and Comunity, Università di Milano, Italy

Adelaide Buora [b]
b Department of Clinical Sciences and Comunity, Università di Milano, Italy

Francesco Scardulla [c]
c Dipartimento di Ingegneria Chimica, Gestionale, Informatica, Meccanica dell'Università degli Studi di Palermo, Universita` degli Studi di Palermo, Italy

Bruno Guerciotti [d]
d MOX, Dipartimento di Matematica, Politecnico di Milano, Italy

Laura Forzenigo [e]
e Radiology Unit, Fondazione I.R.C.C.S. Ca' Granda, Ospedale Maggiore Policlinico di Milano, Italy

Piero Biondetti [e]
e Radiology Unit, Fondazione I.R.C.C.S. Ca' Granda, Ospedale Maggiore Policlinico di Milano, Italy

and

Christian Vergara [d]
d MOX, Dipartimento di Matematica, Politecnico di Milano, Italy.

Corresponding author

Maurizio Domanin
Operative Unit of Vascular Surgery, Fondazione I.R.C.C.S. Ca' Granda Ospedale Maggiore Policlinico di Milano, Italy,
Via Francesco Sforza 35
20122 Milano, Italy.
Tel +39-2-55032438
Email: maurizio.domanin@unimi.it

Original article

Short title

Analysis of WSS indices and closure techniques

What this paper adds

The aim of the study is to analyze how closure technique influences fluid-dynamics after carotid endarterectomy, through a computational comparison of the viscous forces based on patient-specific flow conditions and geometries. We calculated WSS-based indices, namely TAWSS, OSI and RRT, to evaluate the development of hemodynamic conditions related to the risk of restenosis. In our series, all the WSS-based indices suggest that fluid-dynamic conditions more prone to carotid restenosis occur when patch graft is used. Our study suggests that patch closure does not seem to be always more protective from restenosis than direct suture. Elective use of patch should be more recommended.

ABSTRACT

Objectives This study aims at comparing by means of computational fluid-dynamics (CFD) the hemodynamics before and after carotid endarterectomy (CEA), and, after CEA, between patch graft (PG) and direct suture (DS) closures.

Design We analyzed wall shear stress (WSS), velocities, and vorticity before and after CEA, to highlight the effect of surgery on hemodynamics, and time averaged WSS (TAWSS), oscillatory shear index (OSI) and relative residence time (RTT) after CEA to highlight the differences in terms of risk of restenosis between PG and DS.

Methods Thirteen cases underwent CEA for stenosis > 70% and were closed with 9 PG and 4 DS. For each of them we measured the flow with Doppler Ultrasound (DUS) and reconstructed geometries from Magnetic Resonance Angiography (MRA).

Results The mean value of the spatial averaged TAWSS was 1.0 Pa for PG and 1.5 Pa for DS, whereas it was 0.03 for PG and 0.07 for DS in the case of OSI. The percentage areas with low

TAWSS and high OSI resulted wider for PG in comparison to DS (TAWSS: 66.2% for PG and 37.2% for DS; OSI: 10.1% for PG and 3.7% for OSI). RRT values resulted higher in the PG group. In particular, the mean of the averaged-in-space values was 4.4 1/Pa for PG and 1.6 1/Pa for DS, whereas the PA with high RRT were 22.5% and 6.5%, respectively.

Conclusions The carotid regions with percentage area of low TAWSS, high OSI and high RRT were wider in the PG group when compared with DS. Thus, hemodynamic conditions more prone to restenosis were observed for PG. The increase of the cross-section area created by PG could induce flow disturbances with potential consequences on long term outcomes. Selective use of PG should consider specific conditions of the patients.

Keywords: Carotid bifurcation, Carotid endarterectomy, Computational fluid dynamics, Wall shear stress, Finite element method.

Word count: 3912/4000

INTRODUCTION

Carotid bifurcation is a preferential site for the development of atherosclerotic plaque. A major role in this process is given by the blood fluid-dynamics, which produces particular distributions of wall shear stresses (WSS) at bifurcations which could induce the plaque formation [1]. Carotid endarterectomy (CEA) is the most commonly performed surgical treatment to restore the patency of extracranial district. After CEA, closure technique of the carotid still remains a debated major issue. The values of WSS are dependent on individual anatomy [2-4]. Thus, the changes of geometry, due to the removal of the plaque and to the choice of wall reconstruction, could influence WSS and long term biological behavior such as restenosis.

Computational fluid-dynamics (CFD), based on the Finite Element Method, has been proved to be an effective tool to investigate blood flow quantities at the carotid bifurcation. Viscous forces,

focused on WSS-derived parameters, cannot be measured in routine clinical examination, but can be estimated with high grade of accuracy thanks to CFD [5].

The aim of the study was to provide a CFD analysis based on patient-specific geometries and flow conditions aiming at assessing the effect of CEA on hemodynamics and comparing WSS-based indices between two arteriotomy closure techniques, i.e. direct suture (DS) versus patch graft (PG).

Material and methods

Clinical data.

We studied 13 carotids with a degree of stenosis greater than 70% in 12 patients who underwent CEA. Informed consent was obtained in all cases, and the study was approved by the Ethics Committee. The patients were subdivided into two groups, one where a patch insertion was used (PG group, cases 01-09) and another one where a direct suture was performed (DS group, cases 10-13).

The surgeons followed the recommendations of the Carotid Artery Stenosis Consensus conference for grading of the stenosis [6]. In particular, stenosis estimate and peak systolic velocity (PSV) along the internal carotid artery (ICA) were evaluated with Doppler Ultrasound (DUS) as primary parameters. Demographics characteristics and risk factors of the two groups are listed in Tab. 1.

All cases were asymptomatic, one case (8.3%) had a contralateral occlusion of the internal carotid artery and three cases (25.0%) previously underwent contralateral CEA for severe stenosis.

Operative management.

All the 13 CEAs were performed under regional block anesthesia. Standard surgical techniques, including careful dissection before cross clamping, longitudinal arteriotomy, 2.5 X optical magnification and systemic heparin were used. When PG angioplasty was performed, a 6 x 7.5 mm polyester collagen coated vascular patch Ultra thin (Intervascular®, Mahwah, NJ, United States) was chosen. PG or DS were always performed with a 6-0 no absorbable, monofilament Polipropilene suture line (Everpoint™, Ethicon, Somerville, NJ, United States). PG was performed

in 9 interventions (69.2%) considering sex of the patient, internal carotid diameter, localization and extension of the plaque. DS was performed in 4 cases (30.8%); as first choice in 3 cases for localization of the plaque at the bulb and in presence of carotid artery's diameter > 5 mm and in 1 case for progressive patient's discomfort and lack of collaboration in absence of major neurological concerns (case 10). No perioperative complications were observed and no shunts were necessary in our series. During the two years follow-up no cases of restenosis were observed in both groups.

Acquisition of DUS signals and definition of boundary conditions for CFD.

DUS of carotid bifurcations was performed preoperatively with linear 8 MHz probe and iU22 ultrasound scanner (Philips Ultrasound, Bothwell, U.S.A) by an experienced user (MD). In all the cases, the velocities were acquired at the center of the vessel and with a beam-to-flow angle less than or equal to 60°, in order to obtain measures along the longitudinal direction. The sample volume was positioned within the area of greatest stenosis. ICAs were completely sampled through the region of stenosis until the distal end of the plaque was visualized. Velocities were measured 2 cm retrograde from the bifurcation in the common carotid artery (CCA), and 2 cm downstream the bifurcation in the ICA. To generate patient-specific boundary data from DUS measures to be used in the numerical simulations, we proceeded following the methodology reported in our previous work [7]. For the evaluation of PSV, DUS measures were also acquired at the point of maximum stenosis (Tab. 2). DUS was repeated after 1 month to control the surgical result and to record flow velocities for CFD.

Acquisition of radiological images and mesh generation.

Three-dimensional carotid reconstructions were derived from pre- and post-operative Magnetic Resonance Angiography (MRA), which were performed with a 1.5 T Avanto MR scanner (Siemens, Munich, Germany) with sequences and planes described in our previous work [7]. MRA was performed for all the patients both before and one month after CEA. Surface models of the boundary lumen were obtained using a level-set segmentation technique (VMTK http://www.vmtk.org) (Fig. 1). These were converted into volumetric meshes of tetrahedra in view

of CFD simulations (Fig. 2). The sizes of the meshes were set, after a refinement study, to obtain a mesh-independent numerical solution at the stenosis (Tab. 3).

Numerical simulations and fluid-dynamic indices.

Computational studies in human carotids have been performed since two decades but more recently many works have focused on this issue using patient-specific data [8-9]. This is considered a fundamental issue in view of obtaining accurate numerical results [5]. Unsteady numerical simulations for blood fluid-dynamics were performed by means of the academic software LifeV (http://www.lifev.org) and ~~already~~ reported in our previous work [7]. For CFD we chose a rigid wall assumption.

The analyzed CFD quantities were: a) pre and post CEA flow velocity, vorticity and WSS; and b) post CEA time averaged WSS (TAWSS), oscillatory shear index (OSI), and relative residence time (RRT) [2]. The vorticity quantifies the swirling nature of the flow; WSS is the tangential viscous stress caused by blood flow on the arterial wall. PSV, vorticity and WSS were here used to discuss the abnormal fluid-dynamic conditions before CEA and the restoring of physiological conditions after CEA. Indeed, elevated values of these quantities are related to an increased risk of plaque rupture or embolism [5, 10]. TAWSS is the average of WSS over a heartbeat; OSI is a dimensionless parameter that provides a measure of the oscillating nature of WSS. RRT is an emerging fluid-dynamics index that combines TAWSS and OSI. Its distribution is proportional to the residence time of blood near the wall and it is considered a robust indicator to identify regions where WSS is contemporary low and oscillating. TAWSS, OSI and RRT were here used to provide an indication about the risk of restenosis. Indeed, regions with elevated values of OSI and RRT and low values of TAWSS have been recognized at risk of plaque formation [1, 11-15].

RESULTS

We compared the fluid-dynamic differences induced by CEA in all the 13 carotids and their relations to the different closure technique. The accuracy of the numerical code was already tested in our previous study [7].

Comparison between pre and post CEA.

We compared the flow quantities obtained by numerical simulations before and after CEA (Tab. 4).

*Velocity and vorticity***.** We depicted the streamlines of the velocity field at systole for all the 13 cases, both before and after CEA (Figs. 3 and 4). We observed that maximum velocities calculated before CEA are higher than the ones obtained after CEA, due to the presence of severe stenoses (Tab. 4). Before CEA, the stenosis caused the development of systolic disturbed patterns together with pathological acceleration, particularly observable at the level of the carotid bulb and in the ICA region (Fig. 3). After CEA, systolic velocity fields resulted within a physiological range in all the cases. In both groups, streamlines showed a moderate systolic swirling flow prevalently at the bifurcation or in the bulb (Fig. 4). The reduction of maximum vorticity due to CEA was quantified in a range comprised from 70% to 88% in the PG group and from 76% to 91% in the DS group (Tab. 4),

*WSS***.** In all the cases, the maximum systolic WSS computed by CFD was significantly higher before CEA than after CEA (Tab. 4). Combining the results of WSS, velocity and vorticity, we found no significant differences concerning the restoration of the physiological regimes after CEA between the two groups.

Comparison between PG and DS groups post CEA.

TAWSS and OSI. We calculated the spatial average of TAWSS and OSI distributions obtained after CEA (Tab. 5). We also computed the percentage of bifurcation area characterized by TAWSS values below a threshold of 1 Pa and by OSI values above a threshold of 0.2. The results clearly showed that higher TAWSS values and lower OSI values were obtained when DS was chosen, except for case 05 where both TAWSS and OSI are similar to the DS values.

The average values of percentage area with TAWSS < 1 Pa were respectively 57.1 % (range 8.0-91.9) for the PG group and 37.3 % (range 16.6-47.9) for the DS group, while the percentage areas with OSI > 0.02 were respectively 10.1% (range 2.0-16.0) for the PG group and 3.7 % (range 0.9-7.6) for the DS group. We reported OSI and TAWSS distributions for case 05 (Fig. 5).

RRT. We observed that spatial average of RRT distribution obtained after CEA in the PG group was greater than 2 1/Pa in all the cases, except for the case 05, while in DS group we observed lower values (Tab. 5). The mean was 4.4 1/Pa (range 0.5-11.3) in the PG group and 1.6 1/Pa (range 1.0-2.0) in the DS group.

We also computed the mean percentage of area of RRT with a threshold greater than 4.0 1/Pa, that resulted respectively 22.5 % (range 0.1-43.6) in the PG group and 6.5 % (range 1.7-9.8) in the DS group. The whole series of values resulted higher in all the cases of PG group, with values greater from three to four times with respect to DS cases except for case 05 (Tab. 5). In particular, we observed values lower than 10% in all the four cases with DS, values ranging from 10 to 20% in three cases with PG, and values greater than 20% in other five cases with PG (Tab. 5).

In the PG group, distribution of high RRT resulted particularly concentrated at the carotid bulb in five cases (02-04, 07 and 09), at the bifurcation in two cases (06 and 08), and at the ICA in case 01, while low values of RRT were observed just in case 05. In the DS group, we observed higher values of RRT at the bifurcation in three cases (10, 11, 12) and in the bulb and ICA region in case 13 (Fig. 6).

DISCUSSION

Since its introduction in 1965, PG has been advocated to avoid restenosis after CEA. The closure of the longitudinal arteriotomy with DS sometimes allows for the creation of possible technical defect narrowing the lumen and so reproducing the stenosis. Closure of the arteriotomy with PG should

minimize restenosis, intended as development of myointimal hyperplasia within 2 years from the intervention, or recurrent atherosclerosis thereafter [16].

After a long and heated debate [17-19], in 2004 a meta-analysis of seven randomized clinical trials outcomes conducted before 1986 was published [20]. PG was associated with reduced 30-day and long term risk of ipsilateral stroke, stroke, deaths and reduced rates of return to surgery supporting its standard use. Successive update, still endorsing routinary use of PG, declared much less robust results than in the past maintaining just a borderline significant benefit [21]. A recently published trial reported better results for PG with reduction in restenosis rate although no improvements of the clinical outcomes resulted [22]. Restenosis are less detectable in the enlarged arterial lumen of PG, most of them are asymptomatic and therefore their clinical relevance remains unclear. All those considerations have raised doubts on systematic PG suggesting a selective use of it [23-25].

Local fluid-dynamics plays a crucial role in plaque growth. Biologic and molecular changes are mediated by endothelial cells; low and oscillating WSS are associated to monocyte activation, increased vasoconstriction, oxidative stress, higher cellular turnover and apoptosis. This leads to an inflammatory process [11]. Myointimal hyperplasia, the leading cause of restenosis in vascular surgery, is thought to be a reaction of the arterial wall to this mechanical injury [26-28].

Archie et al, using geometrical models derived from the intraoperative measurement of the carotid bifurcations after CEA and venous PG, reported relatively mild WSS [29]. Kamenskiy et al, using CFD in 16 patients submitted to CEA or carotid eversion, observed that PG considerably modifies bifurcation geometries increasing the cross-sectional area and the length of the bulb [30]. After PG wide areas of high OSI and low TAWSS were computed as consequence of abrupt transition of diameter from the PG level to the native artery. Harloff et al, investigating carotid bifurcation with 4D MRA in healthy patients, found that WSS was influenced by the individual carotid geometries [31]. The presence of a severe stenosis changes WSS, whereas CEA of previously high-grade ICA stenosis lead to a reprise of WSS distribution similar to the physiological values observed in healthy

patients. Harrison et al, performing a CFD study on silicone carotid bifurcation models reconstructed from transverse DUS scan, compared DS vs two different PG sizes (5 mm and 8 mm) [32]. They reported that PG did not generate any favorable flow dynamic condition but the tighter patch offered a better hemodynamic behavior than the wider one.

In our study, CFD was firstly used to compare, in stenosis greater than 70%, hemodynamic before and after CEA.

Clinical efficacy of CEA is widely known and admitted but the haemodynamic differences between pre and post surgery conditions have been scarcely investigated. In this study, CFD confirmed the hemodynamic advantages of surgery. Indeed, after CEA we observed, in all the cases, peak velocities, vorticity and WSS reduction, independently of the choice of the closure technique.

About the comparison between PG and DS groups after CEA, the whole series of WSS-based descriptors, which have been recognized as trustable indicators of the development of atheromasic plaque and thus of restenosis, were computed at the bifurcation and at ICA. When DS was performed, the percentage area with TAWSS and OSI respectively lower and higher than thresholds, which are suitable to describe the risk of plaque formation, resulted significantly wider in PG cases compared to DS cases [13].

Both TAWSS and OSI contribute to determine RRT, which quantifies the mass transport of atherogenic substances to the wall increasing the probability of deposition of platelets and macrophages, finally resulting in myointimal hyperplasia. RRT values resulted higher in the PG group, confirming that this closure technique promotes hemodynamic conditions which could increase the risk of restenosis.

By the analysis of every single case, we observed different haemodynamic behaviours. In the PG group, despite the exclusive use of 6 mm patch avoiding larger measures already described as hemodynamically unfavourable [32], in 4 cases (04, 06-08) we did not observe any advantage, with WSS indicator values worse than in DS group. In other four cases (01-03, 09) the effects were even worse because large cross sectional areas were created in the carotid bulb. There was just one case

in PG group (05) where all WSS indicators calculated were within normal ranges and no areas of low TAWSS or high OSI and RRT were present. In this case, the stenosis was localized distal in the ICA region, where the mean vessel diameter could be significantly decreased by DS, so that the choice for PG was in this case correct.

In all the DS cases (10-13) we reported TAWSS, OSI and RRT indices and their distribution patterns. In one case (10), initially intended to PG, we chose intraoperatively to perform DS, shortening cross clamp time, to overcome patient intolerance to loco-regional anesthesia. Despite this problem, case 10 showed just slightly high velocities but the values of TAWSS, OSI and RRT were still included in the range of the other cases of DS without any adverse effect on hemodynamic as we were initially worried.

Cross-checking the results, in the prevalence of the cases here reported, PG could lead to fluid-dynamic conditions with a higher risk of restenosis than DS, which seems instead to be characterized by WSS distributions more spared from risk of restenosis recurrences.

In accordance with other studies, no fluid-dynamic motivations seem to support an extensive use of patch in carotid surgery. Guidelines are favourable to obligatory PG but opinions still differ on the matter [17-18, 24-25]. PG is undoubtedly associated with a series of peri-operative risks, strictly linked to the need of a double stitch with longer times of carotid cross clamp and consequent increased risk for cerebral ischemia and discomfort for the patient when loco-regional anaesthesia is used. Moreover, the insertion of alloplastic material adds risks of suture line bleeding and is subjected to possible severe complications such as infection or pseudo-aneurysm [34]. PG should be performed in selected cases, such as in small diameter ICA, when the arteriotomy extends beyond the bulb segment or when particular technical problems occur during surgery.

Conclusions

CFD allows to obtain accurate quantifications of WSS and related indices, not available with standard ultrasonographic nor radiological investigations. Several studies have demonstrated the role of CFD to identify flow conditions prone to stenosis development. We analysed the hemodynamics before and after CEA and we observed that PG seems to produce some disadvantage in terms of hemodynamic conditions more prone to restenosis with respect to DS. Consequently, the use of PG should be more selective and restricted to particular conditions.

Limitation of this study are related to the absence of any analysis on biological factors that could influence the physiopathologic mechanism of restenosis, to the lack of randomization of treatment in our study and to the absence of any statistical analysis related to the small sample of cases reported.

REFERENCES

1. Ku DN, Giddens DP, Zarins CK, Glagov S. Pulsatile flow and atherosclerosis in the human carotid bifurcation. Positive correlation between plaque location and low oscillating shear stress. Arteriosclerosis 1985; 5:293-302.

2. Lee SW, Antiga L, Spence JD, Steinman DA. Geometry of the carotid bifurcation predicts its exposure to disturbed flow. Stroke 2008; 39:2341-2347

3. Phan TG, Beare RJ, Jolley D, Das G, Ren M, Wong K et al. Carotid artery anatomy and geometry as risk factors for carotid atherosclerotic disease. Stroke. 2012; 43:1596-601.

4. Gallo D, Steinman DA, Morbiducci U. An insight into the mechanistic role of the common carotid artery on the hemodynamics at the carotid bifurcation. Ann Biomed Eng 2015; 43:68-81.

5. Groen HC, Simons L, van den Bouwhuijsen QJ, Bosboom EM, Gijsen FJ, van der Giessen AG et al. MRI-based quantification of outflow boundary conditions for computational fluid dynamics of stenosed human carotid arteries. J Biomech 2010; 43:2332-2338.

6. Grant EG, Benson CB, Moneta GL, Alexandrov AV, Baker JD, Bluth EI et al Carotid Artery Stenosis: Gray-Scale and Doppler US Diagnosis - Society of Radiologists in Ultrasound Consensus Conference. Radiology 2003;229: 340-346.

7. Guerciotti B, Vergara C, Azzimonti L, Forzenigo L, Biondetti P, Domanin M. Computational study of the fluid-dynamics in carotids before and after endarterectomy. Journal of Biomechanics 2015; in press http://dx.doi.org/10.1016/j.jbiomech.2015.11.009i.

8. Campbell IC, Ries J, Dhawan SS, Quyyumi AA, Taylor WR, Oshinski JN. Effect of inlet velocity profiles on patient-specific computational fluid dynamics simulations of the carotid bifurcation. J Biomech Eng 2012; 134:051001

9. Wake AK, Oshinski JN, Tannenbaum AR, Giddens DP. Choice of in vivo versus idealized velocity boundary conditions influences physiologically relevant flow patterns in a subject-specific simulation of flow in the human carotid bifurcation. J Biomech Eng 2009; 131:021013.

10. Stroud JS, Berger SA, Saloner D. Numerical analysis of flow through a severely stenotic carotid artery bifurcation. J Biomech Eng 2002;124:9–20.

11. Malek AM, Alper SL, Izumo S. Hemodynamics shear stress and its role in atherosclerosis. JAMA 1999; 282:2035-2042.

12. Nixon AM, Gunel M, Sumpio BE. The critical role of hemodynamics in the development of cerebral vascular disease. J Neurosurg. 2010; 112:1240-1253.

13. Samady H, Eshtehardi P, McDaniel MC, Suo J, Dhawan SS, Maynard C et al. Coronary artery wall shear stress is associated with progression and transformation of atherosclerotic plaque and arterial remodeling in patients with coronary artery disease. Circulation 2011;124:779 – 788.

14. Himburg HA, Grzybowski DM, Hazel AL, LaMack JA, Li XM, Friedman MH. Spatial comparison between wall shear stress measures and porcine arterial endothelial permeability. Am J Physiol Heart Circ Physiol 2004; 286:H1916-1922.

15. Morbiducci U, Ponzini R, Rizzo G, Cadioli M, Esposito A, Montevecchi FM et al. Mechanistic insight into the physiological relevance of helical blood flow in the human aorta: an in vivo study. Biomech Model Mechanobiol, 2011; 10:339–355.

16. Imparato AM. The role of patch angioplasty after carotid endarterectomy. J Vasc Surg 1988; 7:715-716.

17. Golledge J, Cuming R, Davies AH, Greenhalgh RM. Outcome of selective patching following carotid endarterectomy. Eur J Vasc Endovasc Surg 1996; 11:458-463.

18. Pappas D, Hines GL, Yoonah Kim E. Selective patching in carotid endarterectomy: is patching always necessary? J Cardiovasc Surg 1999; 40:555-559.

19. Rockman CB, Halm EA, Wang JJ, et al. Primary closure of the carotid artery is associated with poorer outcomes during carotid endarterectomy. J Vasc Surg 2005; 42:870–877.

20. Bond R, Rerkasem K, AbuRahma AF, Naylor AR, Rothwell PM. Patch angioplasty versus primary closure for carotid endarterectomy. Cochrane Database Syst Rev 2004: CD000160.

21. Rerkasem K, Rothwell PM. Systematic review of randomized controlled trials of patch angioplasty versus primary closure and different types of patch materials during carotid endarterectomy. Asian J Surg 2011; 34:32-40.

22. Malas M, Glebova NO, Hughes SE, Voeks JH, Qazi U, Moore WS et al. ,Effect of patching on reducing restenosis in the carotid revascularization endarterectomy versus stenting trial. Stroke. 2015; 46:757-761. doi: 10.1161/STROKEAHA.114.007634. Epub 2015 Jan 22.

23. Mannheim D, Weller B, Vanhadim E, Karmely R. Carotid endarterectomy with a polyurethane patch versus primary closure: a prospective randomized study. J Vasc Surg 2005; 41:403–408.

24. Cikrit DF, Larson DM, Sawchuk AP, Thornhill C, Shafique S, Nachreiner RD et al. Discretionary carotid patch angioplasty leads to good results. Am J Surg 2006;1 92:e46-e50.

25. Zenonos G, Lin N, Kim A, Kim JE, Governale L, Friedlander RM. Carotid endarterectomy with primary closure: analysis of outcomes and review of literatures. Neurosurgery 2012; 70:646-655.

26. Clowes AW, Reidy MA, Clowes MM. Mechanisms of stenosis after arterial injury. Lab Invest 1983; 49:208-215.

27. Mattsson EJ1, Kohler TR, Vergel SM, Clowes AW. Increased blood flow induces regression of intimal hyperplasia. Arterioscler Thromb Vasc Biol 1997; 17:2245-2249.

28. Kamenskiy AV, MacTaggart JN, Pipinos II, Gupta PK, Dzenis Y.A. Hemodynamically motivated choice of patch angioplasty for the performance of carotid endarterectomy. Ann. Biomed Eng 2013; 41:263-278.

29. Archie JP Jr. Geometric dimension changes with carotid endarterectomy reconstruction. J Vasc Surg 1997; 25:488-498.

30. Kamenskiy AV, Pipinos II, Dzenis YA, Gupta PK, Jaffar Kazmi SA, MacTaggart JN. A mathematical evaluation of hemodynamic parameters following carotid eversion and conventional patch angioplasty. Am J Physiol Heart Circ Physiol 2013; 305:H716–H724 doi:10.1152/ajpheart.00034.2013.

31. Harloff A, Berg S, Barker AJ, Schöllhorn J, Schumacher M, Weiller C, et al. Wall shear stress distribution at the carotid bifurcation: influence of eversion carotid endarterectomy. Eur Radiol 2013; 23:3361–3369 DOI 10.1007/s00330-013-2953-4.

32. Harrison GJ, How TV, Poole RJ, Brennan JA, Naik JB, Vallabhaneni SR. Closure technique after carotid endarterectomy influences local hemodynamics, J Vasc Surg 2014; 60,418–427.

33. Naylor AR, Payne D, London NJM, Thompson MM, Dennis MS, Sayers RD et al. Prosthetic Patch Infection After Carotid Endarterectomy. Eur J Vasc Surg 2002; 23:11-16.

TABELS

Tab.1 – Patient demographic characteristics and risk factors

			Patch				Direct suture		
			Average	SD	(%)		Average	SD	(%)
Age		years	72.88	6.33			70	12.73	
Sex									
Males			3		(37,5)		2		(50.0)
Females			5		(62,5)		2		(50.0)
Weight		Kg	58.75	12.0		73.75	17.1		
Height		cm	1.62	0.6		1.73	0.17		
Body mass Index				22.33	4.71		24.42	2.6	
Risk factors									
Smoke			5		(62,5)		2		(50.0)
Dislipidemia			4		(50.0)		4		(100)
Hypertension			8		(100)		4		(100)
Diabetes			3		(37,5)		2		(50.0)
CHD			1		(12,5)		2		(50.0)
Side		Right	3				1		
		Left	4				3		
		Bilateral	1				0		

Tab. 2 Location of the stenosis (CCA Common Carotid Artery, B Bulb, ICA Internal Carotid Artery), carotid plaque characteristics (L Lipidic, FL Fibrolipidic, F Fibrous, FCA Fibro-calcific, CA Calcific) and Duplex scan values of the peak of systolic velocity (PSV).

Patient	Closure technique	Location	Plaque characteristics	Maximum stenosis PSV (cm/sec)
01	PG	CCA , B	FCA	375
02	PG	B	F	300
03	PG	B, ICA	CA	280
04	PG	B, ICA	CA	300
05	PG	ICA	FCA	372
06	PG	B	F	350
07	PG	B, ICA	F	200
08	PG	B	FCA	270
09	PG	B, ICA	FCA	240
10	DS	B	CA	220
11	DS	B, ICA	CA	280
12	DS	CCA, B, ICA	FL	200
13	DS	B	L	200

Tab. 3 Number of tetrahedra for numerical simulation derived from segmentation of MRA imaging

CASE	CLOSURE TECHNIQUE	Before CEA (number of tethraedra)	After CEA (number of tethraedra)
01	PG	270 000	130 000
02	PG	260 000	100 000
03	PG	320 000	180 000
04	PG	240 000	200 000
05	PG	560 000	170 000
06	PG	310 000	240 000
07	PG	510 000	660 000
08	PG	470 000	380 000
09	PG	390 000	450 000
10	DS	510 000	310 000
11	DS	790 000	260 000
12	DS	700 000	350 000
13	DS	650 000	240 000

Tab. 4 Systolic maximum WSS and vorticity values computed by CFD before and after CEA.

Case	Closure technique	Before CEA Maximum systolic vorticity (1/s)	After CEA Maximum systolic vorticity (1/s)	Before CEA Maximum systolic WSS (Pa)	After CEA Maximum systolic WSS (Pa)
01	PG	10 946	2 154	37.4	4.5
02	PG	6 794	948	29.4	3.5
03	PG	14 852	3 764	49.7	5.0
04	PG	10 238	3 004	35.8	6.7
05	PG	61 200	7 200	200	23.0
06	PG	31 400	4 270	102	14.7
07	PG	11 100	3 230	35.3	11.0
08	PG	12 100	2 130	40.8	7.0
09	PG	16 800	4 750	56.1	14.0
10	DS	11 955	2 442	72.1	8.3
11	DS	15 060	1 287	49.8	5.0
12	DS	10 575	2 429	64.5	21.3
13	DS	8 933	2 090	74.7	9.2

Tab. 5 TAWSS, OSI and RTT values computed by CFD after CEA.

Case	Closure technique	Averaged in space TAWSS (Pa)	Area below threshold TAWSS < 1 Pa (%)	Averaged in space OSI	Area above threshold OSI > 0.2 (%)	RRT Averaged in space (1/Pa)	Area above threshold RRT > 4 1/Pa (%)
01	PG	0.5	82.7	0.09	11.6	5.7	34.6
02	PG	0.4	91.9	0.09	15.7	11.3	43.6
03	PG	0.5	82.5	0.07	10.4	7.2	35.8
04	PG	0.8	70.2	0.06	9.0	3.6	16.2
05	PG	3.8	8.0	0.02	2.0	0.5	0.1
06	PG	1.0	52.0	0.09	16.0	2.2	13.0
07	PG	0.9	48.0	0.07	7.8	2.9	16.0
08	PG	0.7	37.0	0.06	6.0	2.9	20.0
09	PG	1.0	41.6	0.09	13.0	3.2	23.0
10	DS	1.1	45.0	0.02	0.9	1.0	1.7
11	DS	1.6	47.9	0.06	5.1	1.8	6.8
12	DS	2.0	16.6	0.03	1.5	1.8	8.0
13	DS	1.3	39.6	0.04	7.6	2.0	9.8

FIGURES CAPTION LIST

Fig. 1 Example of surface models of the carotid bifurcation (case 05 before CEA);

Fig. 2 Examples of mesh derived from MRI segmentation (case 06 before and after CEA).

Fig. 3 Velocity field streamlines in the PG group (cases 01-09) and DS group (cases 10-13). On the left: before CEA; on the right: after CEA.

Fig. 4 Plot examples of TAWSS and OSI distribution calculated after CEA (case 06).

Fig. 5 Plot of RRT distribution calculated in the PG group (cases 01-09) and DS group (cases 10-13) after CEA .

Figure 1

Figure 2

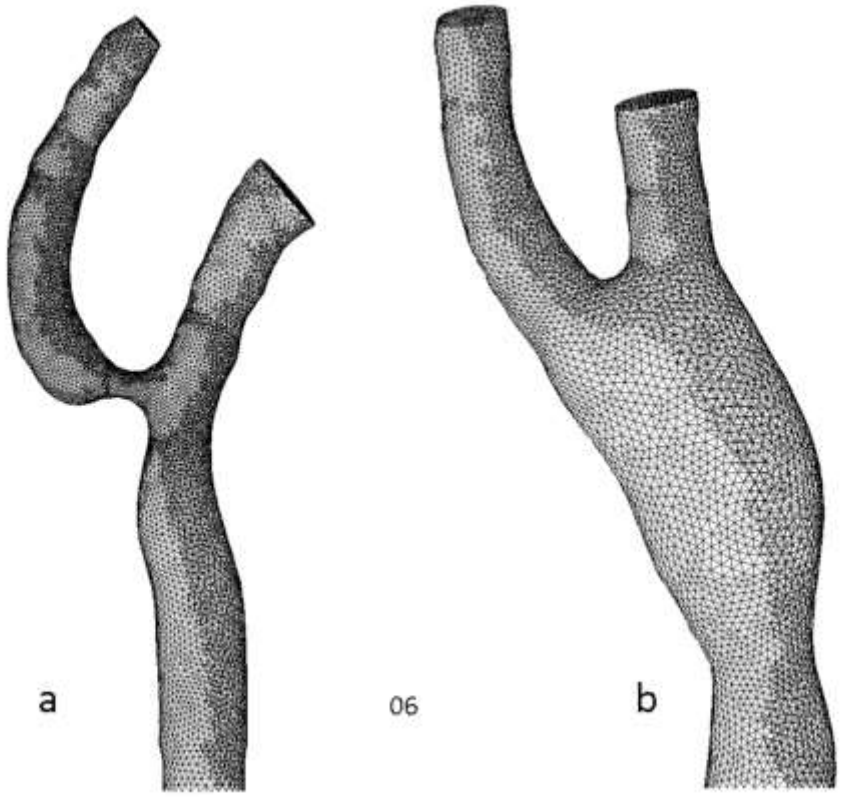

Figure 3

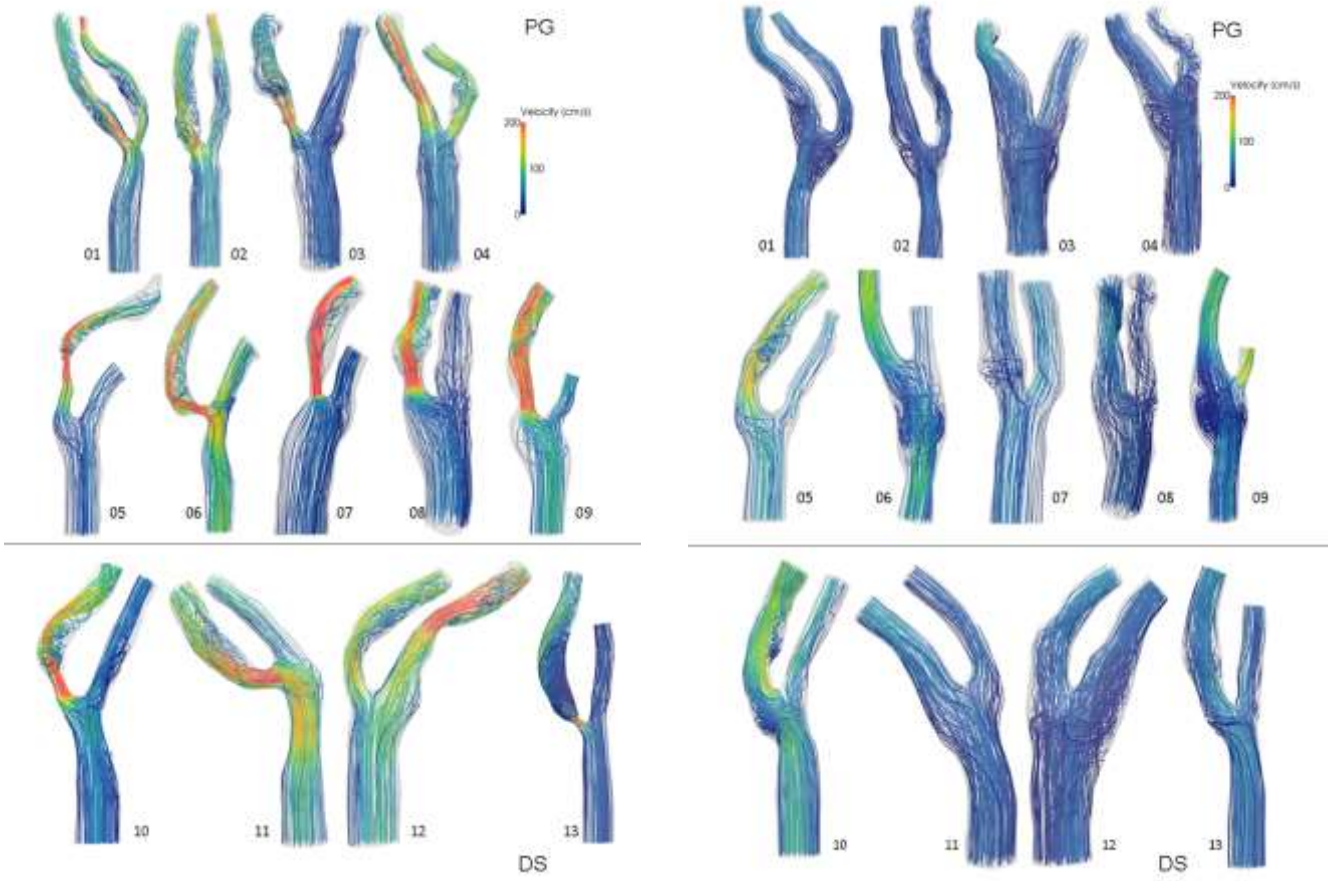

Figure 4

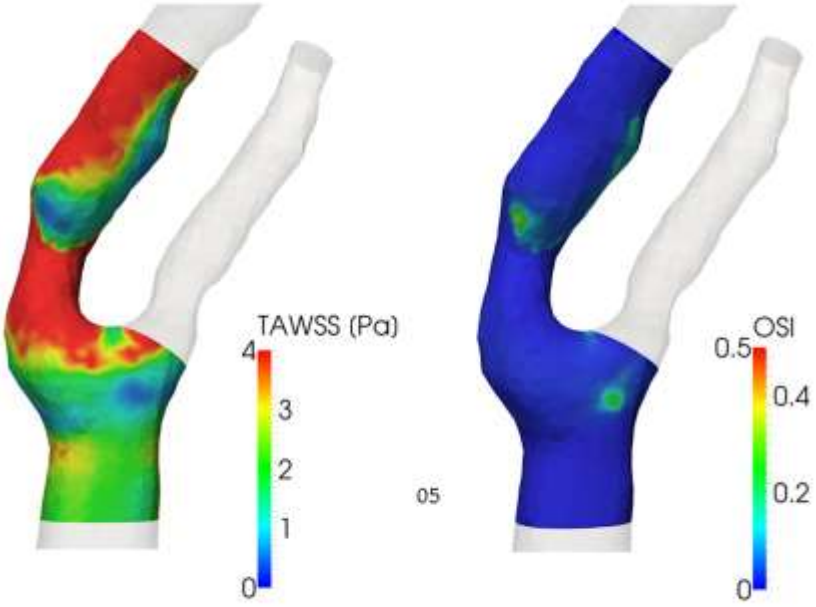

Figure 5

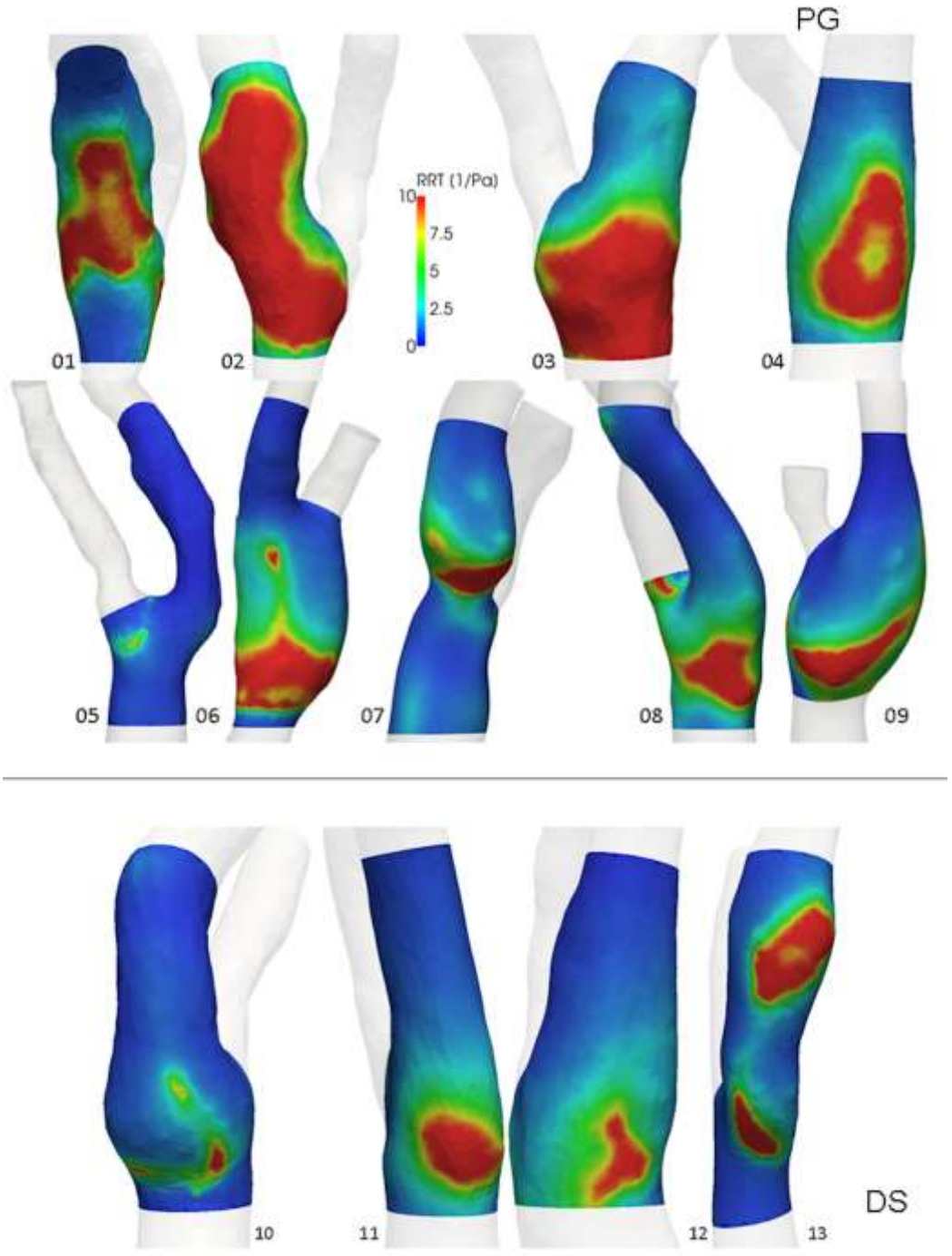

MOX Technical Reports, last issues

Dipartimento di Matematica
Politecnico di Milano, Via Bonardi 9 - 20133 Milano (Italy)

63/2015 Lancellotti, R.M.; Vergara, C.; Valdettaro, L.; Bose, S.; Quarteroni, A.
Large Eddy Simulations for blood fluid-dynamics in real stenotic carotids

62/2015 Signorini, M.; Zlotnik, S.; Díez, P.
Proper Generalized Decomposition solution of the parameterized Helmholtz problem: application to inverse geophysical problems.

61/2015 Tagliabue, A.; Dedè, L.; Quarteroni, A.
Fluid dynamics of an idealized left ventricle: the extended Nitsche's method for the treatment of heart valves as mixed time varying boundary conditions

60/2015 Perotto, S.; Reali, A.; Rusconi, P.; Veneziani, A.
HIGAMod: A Hierarchical IsoGeometric Approach for MODel reduction in curved pipes

59/2015 Menafoglio, A.; Guadagnini, A.; Secchi, P.
Stochastic Simulation of Soil Particle-Size Curves in Heterogeneous Aquifer Systems through a Bayes space approach

58/2015 Iapichino, L.; Rozza, G.; Quarteroni, A.
Reduced basis method and domain decomposition for elliptic problems in networks and complex parametrized geometries

57/2015 Wilhelm, M.; Dedè, L.; Sangalli, L.M.; Wilhelm, P.
IGS: an IsoGeometric approach for Smoothing on surfaces

54/2015 Canuto, C.; Nochetto, R. H.; Stevenson, R.; Verani, M.
Adaptive Spectral Galerkin Methods with Dynamic Marking

55/2015 Fumagalli, A.; Zonca, S.; Formaggia, L.
Advances in computation of local problems for a flow-based upscaling in fractured reservoirs

56/2015 Bonaventura, L.; Della Rocca, A.
Monotonicity, positivity and strong stability of the TR-BDF2 method and of its SSP extensions